Geomech. Geophys. Geo-energ. Geo-resour. (2022)8:40
https://doi.org/10.1007/s40948-022-00348-8

ORIGINAL ARTICLE

A transient dual porosity/permeability model for coal multiphysics

Yifan Huang · Jishan Liu · Derek Elsworth · Yee-Kwong Leong

Received: 13 June 2021 / Accepted: 8 January 2022

Abstract Conventional dual porosity/permeability models for coal cannot capture the true transient nature of matrix-fracture mechanical interactions because these interactions are normally characterized through two equilibrium systems within the same REV (representative elementary volume). In this study, the transient process in the matrix system is included through the embedment of a local REV structure into the overall multiphysics formulation. This inclusion transforms conventional dual porosity/permeability equilibrium models into non-equilibrium ones. Consequently, coal permeability evolves from initial to final equilibrium within the REV. Equilibrium models represent two end points (initial and final equilibrium) while our new model represents the evolution of coal permeability between these two end points. The model is verified against experimental observations of coal permeability under common experimental conditions of constant confining pressure and constant effective stress. Our results show that conventional equilibrium models underestimate the role of coal matrix or matrix-fracture mechanical interactions, that current experimental observations represent only a small portion of the complete evolution process, and that as a tool of knowledge extension our model extends the experimental observations to a representation of the coal permeability whole evolution process from initial to ultimate equilibrium.

Article Highlights

(1) Through the embedment of a local REV structure into the overall multiphysics formulation, the transient/non-equilibrium process in the matrix system is considered.
(2) Conventional dual porosity/permeability models for coal are modified to capture the true transient nature of the matrix-fracture interaction.
(3) The whole evolution process of coal permeability from initial to ultimate equilibrium is represented.

Keywords Coal permeability · Matrix-fracture interaction · Local structure · Dual porosity · Non-equilibrium

Y. Huang · J. Liu (✉) · Y.-K. Leong
Department of Chemical Engineering, School of Engineering, The University of Western Australia, 35 Stirling Highway, Perth, WA 6009, Australia
e-mail: jishan.liu@uwa.edu.au

D. Elsworth
Department of Energy and Mineral Engineering, G3 Centre and Energy Institute, The Pennsylvania State University, University park, PA 16802, USA

Published online: 07 February 2022

1 Introduction

In recent years, unconventional gas reservoirs, such as coalbed methane (CBM), have attracted attention from various countries due to their huge reserves of methane as a fuel and the advantage of improving the energy structure (Tan et al. 2011; Pan et al. 2012; Peng et al. 2017). As a key factor controlling gas extraction, permeability is affected by complex interactions of stress and sorptive chemistry, and changes during gas production (Liu et al. 2011a; Moore 2012; Chen et al. 2009). Fully understanding the transient characteristics of permeability evolution is the key to improving productivity of CBM (Zhang et al. 2008).

Although great efforts have been made and a broad array of permeability models have been proposed in past decades (Warren 1963; Gray 1987; Palmer 1996; Zhao et al. 2004; Shi, et al. 2005; Cui et al. 2005; Zhang et al. 2008; Wu et al. 2010; Liu et al. 2011c), these models have not been able to fully explain the results of laboratory measurements (Liu et al. 2011b; Wei et al. 2019a, b ; Siriwardane 2009; Chen et al. 2011; Wang et al. 2016; Feng et al. 2017). These experimental observations are normally conducted under constant effective stresses (CES) and constant confining pressure (CCP). Based on the results of previous models, as gas injection pressure rises, permeability should remain unchanged for CES, while, for CCP, it should increase. However, these model predictions contradict with the experimental observations where permeability ratios change within an upper envelope (corresponding to the solution of free-swelling) and a lower envelope (corresponding to the solution of zero-swelling) (Shi et al. 2018).

Several approaches have been developed to address these contradictions. Some scholars derived permeability models under specific boundary conditions, such as the uniaxial strain, but they do not match well with actual experimental conditions (Shi et al. 2014; Shi et al. 2018). In addition, a strain-splitting approach was proposed (Liu et al. 2010). The internal swelling strain is divided into two parts: one for coal and the other for fractures. In this approach, only the latter one is considered as responsible for the variation of permeability. However, it is difficult to define the physical meaning of the strain splitting factor. In 2011, the fundamental reason was identified as matrix-fracture mechanical interactions (Liu, et al. 2011a; 2011b). Because of a high contrast of permeability between matrix and fractures, fracture pressure reaches injection pressure instantaneously, while the gas diffusion from fractures to matrix lasts for an extended period, potentially from a few months to years (Liu, et al, 2011b). With gas diffusion, matrix deforms non-uniformly (from local to global swelling), and this transient process in matrix results in the matrix-fracture mechanical interaction that changes the fracture volume and coal permeability (Qu, et al. 2014). Previous models (defined as equilibrium models) are derived under the local equilibrium assumption between matrix and fractures, and the transient process in matrix is ignored. Therefore, they represent permeability only at the initial (prior to gas injection) and ultimate (fully invaded) equilibrium state, while the permeability evolution between these two end points is simply not considered (Peng et al. 2014; Zeng et al. 2020). However, experimental data were normally measured under non-equilibrium states (Wei, et al. 2019a; Shi, et al. 2020). These previous studies suggest that the local equilibrium assumption is responsible for the contradictions between theoretical projections and experimental observations.

As one of the computationally efficient and widely used methods for simulating the fluid flow in coal, conventional dual porosity/permeability models treat coal as two media: matrix and fractures (Barenblatt et al. 1960; Warren et al. 1963). The REV with two systems is incorporated into a single mathematical point (no spatial information) instead of a physical point (Zhang et al, 2018; Wei et al, 2019b). The mass transport behavior is based on the pseudo steady state (Ranjbar et al. 2011). That means that the two systems in the REV are regarded to be in equilibrium states and the gas diffusion within matrix cannot be accounted for (Abbasi et al. 2019). Under this condition, the matrix-fracture interaction is only characterized by two equilibrium systems in the REV instead of the true transient nature (Peng et al. 2014; Cao et al. 2016; Wei et al. 2016; Zhang et al. 2018). Although some approaches were proposed, such as the transient approach that derives shape factors by solving the diffusivity equation, and Multiple Interacting Continua (MINC) that subdivides matrix into multiple-interacting-continua, to consider the gas diffusion within matrix in the dual porosity/permeability approach, they are mainly to improve the accuracy of the matrix-fracture mass transfer (Lim, et al. 1995; Wu, et al. 1988; Farah, et al. 2019). However, the more

important matrix-fracture mechanical interactions caused by the transient processes within the matrix are still not considered.

As reviewed above, conventional dual porosity/permeability models do not consider the transient nature of an individual process such as diffusion within an REV. The REV is treated as a mathematical construct rather than a physical entity. For low permeability coal, this may result in significant inconsistencies between conventional theory and laboratory & field observations. In this study, the theoretical deficiency has been addressed through the embedment of a local REV structure into the overall multiphysics formulation. This inclusion has transformed conventional dual porosity/permeability equilibrium models into non-equilibrium ones. Consequently, coal permeability evolves also from initial to final equilibrium. Equilibrium models represent two end points (initial and final equilibrium) while our new model represents the evolution of coal permeability between these two end points.

2 Conceptual model

2.1 Transient dual porosity/permeability approach

Since the REV is treated as a single mathematical point that does not have any length, area, or volume, as shown in Fig. 1, in the conventional dual porosity/permeability approach, the spatial information is lost (Wei et al. 2019b). The state parameters, such as pressure and strain, within each representative point of the matrix (i.e., the simulation cell for matrix) can only be regarded to be uniform. Consequently, the process of gas diffusion within the matrix and the corresponding non-uniform deformation of the matrix cannot be characterized (Wei et al. 2019b). In order to address the theoretical deficiency, in this study, we propose a transient dual porosity/permeability approach, in which the relationship between the representative point of the matrix in the conventional dual porosity/permeability approach and the actual matrix block in the REV is established through a pressure mapping method, as shown by the orange part in Fig. 1. The premise of this method is that pressure in the representative point of the matrix is consistent with average pressure of the matrix block. This means we

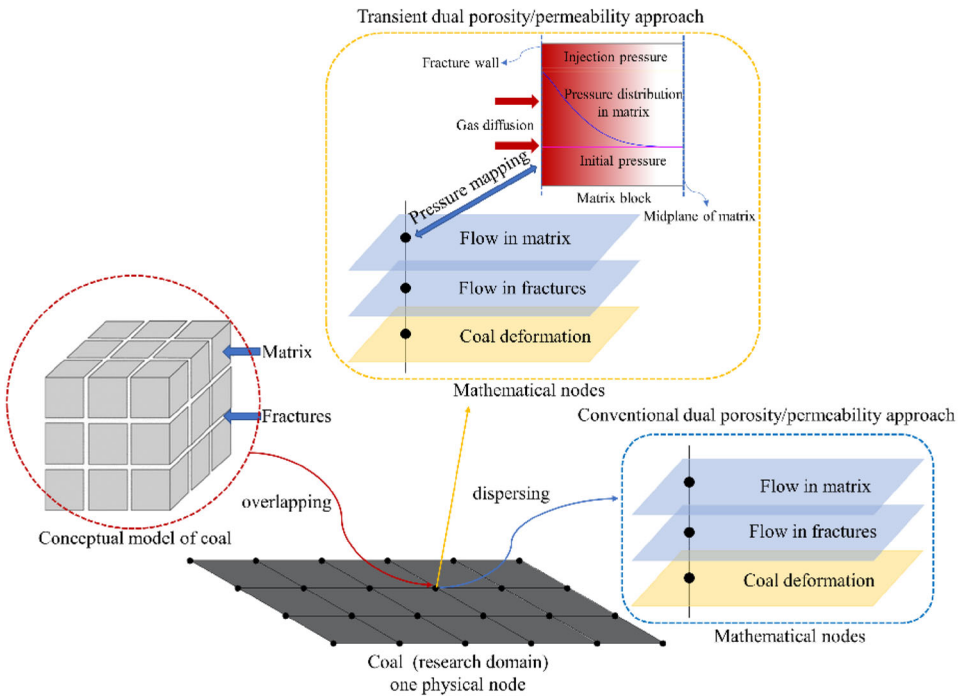

Fig. 1 Illustration of the dual porosity/permeability approach (after Zhang et al. 2018)

use the conventional dual porosity/permeability approach to calculate pressure for each representative point of the matrix, and the obtained quantities are treated as average pressure for the matrix block in the REV. In the matrix block, the pressure distribution and associated matrix non-uniform deformation can be considered. Therefore, in the proposed approach, there are two systems, one of which is the conventional dual porosity/permeability approach (defined as the global system), the other is the actual matrix block (defined as the local system). We employ the subscripts g and l to distinguish parameters as well as equations in the two systems, respectively. If parameters are not distinguished by subscripts, it means that they are constants and are identical in the two systems. In summary, the proposed approach is a continuous approach with an embedded local microstructure.

As a complex porous medium, the matrix exhibits strong heterogeneity and anisotropy. The evaluation of the gas diffusion within the matrix block is difficult but feasible to treat with some simplifications and assumptions (Berre et al. 2019). In this study, the matrix block (i.e., the local system) is regarded as the simplest plausible physical model: one-dimensional pressure diffusion from a cuboid region with the fracture wall as base and the length of half matrix spacing as height (Patzek et al. 2013, 2014). Therefore, the pressure distribution within the matrix block can be calculated through solving the one-dimension diffusion equation. To arrive at a specific linear diffusion problem and solve the problem with closed-form expressions, some assumptions need to be made: (1) gas contained within the matrix block is ideal, and viscosity is constant; (2) the matrix block is saturated by gas; (3) permeability and porosity are uniform and unchanged; (4) the effect of gas adsorption on the pressure distribution is neglected (Patzek et al. 2014). Based on these assumptions, a linear diffusion equation is (Bear 2013)

$$\frac{\partial^2 p_l}{\partial x_l^2} = \frac{\varphi_{m_0}\mu c_t}{k_{m_0}}\frac{\partial p_l}{\partial t_l} \tag{1.1}$$

$$p_l|_{x_l=0} = p_{gf}(t_g) \tag{1.2}$$

$$\left.\frac{\partial p_l}{\partial x_l}\right|_{x_l=L} = 0 \tag{1.3}$$

$$p_l|_{t_l=0} = p_i \tag{1.4}$$

where p_l is pressure in the matrix block; φ_{m_0} and k_{m_0} are the initial matrix porosity and permeability; μ is gas viscosity; c_t is gas compressibility; p_i is initial pressure; $x_l = 0$ refers to the fracture wall; $x_l = L$ refers to half-length of matrix spacing; p_{gf} is fracture pressure in the dual porosity/permeability approach, which changes with the time of the global system rather than that of the local system.

Through solving diffusion equation (Eq. 1.1) with boundary conditions (Eqs. 1.2 and 1.3) and the initial condition (Eq. 1.4), the average pressure and pressure distribution within the matrix block can be described as

$$\overline{p_l}(t_l) = \sum_{n=0}^{\infty}\frac{8\left(p_i - p_{gf}(t_g)\right)}{[(2n+1)\pi]^2}e^{-\left[\left(\frac{(2n+1)\pi}{2L}\right)^2\frac{k_{m_0}}{\varphi_{m_0}\mu c_t}\right]t_l} + p_{gf}(t_g) \tag{2}$$

$$p_l(x_l, t_l) = \sum_{n=0}^{\infty}\frac{4\left(p_i - p_{gf}(t_g)\right)}{(2n+1)\pi}e^{-\left[\left(\frac{(2n+1)\pi}{2L}\right)^2\frac{k_{m_0}}{\varphi_{m_0}\mu c_t}\right]t_l}\cdot \sin\frac{(2n+1)\pi x_l}{2L} + p_{gf}(t_g) \tag{3}$$

where $\overline{p_l}$ is the average pressure in the matrix block.

As mentioned above, the average pressure in the matrix block $\overline{p_l}$ is equal to pressure of the representative point of the matrix p_{gm}. Therefore, after inputting p_{gf} and p_{gm} into Eq. 2, the characteristic time t_l can be calculated. After substituting t_l into Eq. 3, we obtain the pressure distribution within the matrix block under specified conditions.

2.2 Concept of the non-equilibrium coefficient

For a homogeneous and isotropic REV under constant confining stress, the strain at each point is the same and equal to the bulk strain if gas pressure is distributed uniformly within the REV. However, as mentioned previously, this conclusion is only applicable to the coal matrix at equilibrium states, while in non-equilibrium states, the matrix deformation is non-uniform, causing the strain at each point to deviate from the bulk strain (Wei et al. 2019b). The strain at different points would change with time and space until pressure anywhere is equalized. In this process, the bulk strain is also a function of time until the

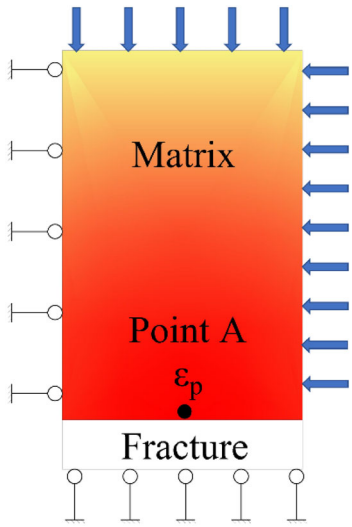

Fig. 2 Illustration of coal with an explicitly expressed fracture

equilibrium state is reached. In this section, we use a model with an embedded fracture to conceptualize the concept, as shown in Fig. 2. Note that the matrix in Fig. 2 is the local system embedded into the overall multiphysics, in which the gas distribution can be expressed as Eq. 3. We choose a point closest to the fracture in the matrix and assume that the pressure at this point is identical to the fracture pressure. The strain at this point is defined as ε_{lp} while the bulk strain is defined as ε_{lm}. We use the volumetric average to calculate the bulk strain, and the strain at different points in the local system can be described as (Zhang et al. 2008)

$$\varepsilon_{linv}(x_l, t_l) = -\frac{\overline{\sigma} - \alpha_m p_l(x_l, t_l)}{K_m} + \varepsilon_{ls} \tag{4}$$

where $\overline{\sigma} = -\sigma_{kk}/3$ is the mean compressive stress; ε_{linv} is the strain at each point in the matrix block; α_m is the Biot coefficient of matrix; K_m is the bulk modulus of matrix; ε_{ls} is the adsorption-induced strain at each point, which can be expressed as:

$$\varepsilon_{ls} = \frac{\varepsilon_L p_l(x_l, t_l)}{p_l(x_l, t_l) + p_L} \tag{5}$$

where ε_L is the Langmuir adsorption constant; p_L is the Langmuir pressure constant.

Combining Eq. 3, 4 and 5, ε_{lp} can be calculated directly and ε_{lm} is obtained through integration. The non-equilibrium coefficient, γ, is introduced, which is defined as

$$\gamma = \frac{\varepsilon_{lp}}{\varepsilon_{lm}} = \frac{\varepsilon_{lp}}{\frac{1}{V_{lm}} \iiint \varepsilon_{linv}(x_l, t_l) dV_{lm}} \tag{6}$$

where V_{lm} is the matrix block volume in the local system.

Prior to gas injection, coal is in an initial equilibrium state, and γ equals unity. Once gas is injected, gas fills fractures instantaneously, while gas diffusion into the matrix block only occurs close to the fracture wall. Beyond this area, pressure basically remains unchanged, and so does the corresponding deformation. Therefore, ε_{lp} increases while changes in ε_{lm} are minor, resulting in an increase of γ. With the gas diffusion, gas propagates throughout the whole matrix block and the swelling area would enlarge, that is, ε_{lm} continually increases. Meanwhile, since fracture pressure gradually reaches injection pressure, ε_{lp} would reach an asymptote. Consequently, γ would drop after reaching the peak. Eventually, when pore pressure is the same as injection pressure everywhere, the ultimate equilibrium state is reached, and the matrix deformation is uniform. That means, ε_{lp} is consistent with ε_{lm}, and γ is equal to unity again. The evolutions of ε_{lm}, ε_{lp} and associated γ during gas injection are shown in Fig. 3. In summary, γ is a function of the matrix strain distribution and reflects the degree of the non-uniform deformation of the matrix.

3 Formulation of the conceptual model

3.1 governing equations for coal deformation

As a typical dual porous medium, coal consists of matrix and fractures, and each component contributes to the coal deformation. According to the traditional poroelastic theory and an analogy between thermal contraction and adsorption swelling, the constitutive relation for the coal deformation with the inclusion of sorption-induced deformation can be defined as Navier-type (Peng, et al. 2014):

$$\begin{aligned} &Gu_{gi,kk} + \frac{G}{1-2v} u_{gk,ki} - \alpha_m p_{gm,i} - K\left(1 - \varphi_{gf_0}\right)\varepsilon_{gms,i} \\ &\quad -\alpha_f p_{gf,i} - K\varphi_{gf_0}\varepsilon_{gfs,i} + f_{gi} = 0 \end{aligned} \tag{7}$$

where m and f denote matrix and fractures respectively; $G = E/2(1+v)$, $K = E/3(1-2v)$,

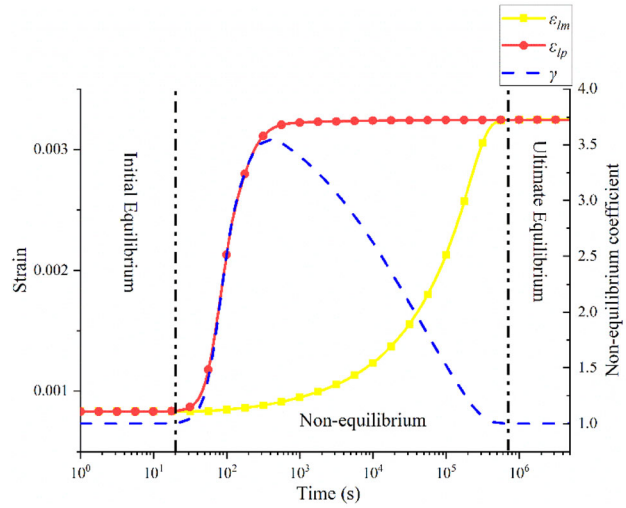

Fig. 3 Evolutions of ε_{lm}, ε_{lp} and γ during gas injection

$a_m = 1 - K_m/K_s$, $a_f = 1 - K/K_m$; G is shear modulus of coal; $u_{g,i}$ is solid frame displacement vector in the global system; v is Poisson's ratio; φ_{gf_0} is the initial fracture porosity; p_g is gas pressure in the global system; K is coal bulk modulus of coal; K_s is the bulk modulus of grains; ε_{gs} is the gas sorption-induced strain; f_g is the body force.

According to the Langmuir adsorption isotherm, the gas sorption-induced strain of matrix and fractures can be expressed:

$$\varepsilon_{gms} = \frac{\varepsilon_L p_{gm}}{p_L + p_{gm}} \tag{8}$$

$$\varepsilon_{gfs} = \frac{\varepsilon_L p_{gf}}{p_L + p_{gf}} \tag{9}$$

3.2 governing equations of gas flow in matrix and fractures

The equation for mass balance of gas in fractured coal can be described as:

$$\frac{\partial m_g}{\partial t_g} + \nabla \cdot (\rho_g q_g) = Q_{gs} \tag{10}$$

where ρ_g is the gas density; $q_g = -\frac{k_g}{\mu}\nabla p_g$ is the Darcy velocity vector; Q_{gs} is the gas source or sink; m_g is the gas mass including free-phase and adsorbed-phase, and can be defined as:

$$m_g = \rho_g \varphi_g + \rho_s \rho_c \frac{V_L p_g}{p_g + p_L} \tag{11}$$

where ρ_s is the gas density at standard conditions; ρ_c is the coal density; V_L is the Langmuir volume constant.

According to the ideal gas law, the gas density is described as

$$\rho_g = \frac{M_{mg}}{RT} p_g \tag{12}$$

where M_{mg} is the molecular mass of the gas, R is the universal gas constant, and T is the absolute gas temperature. Therefore, the gas density in the coal can be expressed as:

$$\rho_g = \frac{p_g}{p_b} \rho_s \tag{13}$$

where p_b is one atmosphere of pressure.

Based on previous studies, coal permeability generally is related to fractures (Liu, et al. 2011c; Pan et al. 2012). According to the definition of coal porosity, the following expression can be obtained (Liu, et al. 2011b; Cheng, 2016):

$$\frac{\Delta \varphi_{gf}}{\varphi_{gf_0}} = \frac{\Delta V_{gf}}{V_{gf_0}} - \frac{\Delta V_{gb}}{V_{gb_0}} \tag{14}$$

where V_{gf} is the fracture volume; V_{gb} is the coal volume.

Under the non-equilibrium state, changes in the fracture volume consist of two components: one is due to the fracture uniform deformation, the other is due to

the matrix-fracture mechanical interaction. Consequently, we obtain the relationship as.

$$\frac{\Delta\varphi_{gf}}{\varphi_{gf_0}} = \frac{\Delta V_{gf}^{int}}{V_{gf_0}} + \frac{\Delta V_{gf}^{uni}}{V_{gf_0}} - \frac{\Delta V_{gb}}{V_{gb_0}} = \Delta\varepsilon_{gf}^{int} + \frac{\alpha_f}{\varphi_{gf_0}}\Delta\varepsilon_{gf}^{e} \tag{15}$$

where V_{gf}^{int} is the fracture volume change induced by the mechanical interaction; V_{gf}^{uni} is the fracture volume change induced by the fracture uniform deformation; ε_{gf}^{e} is the coal effective strain, and can be calculated by (Zhang et al. 2008):

$$\Delta\varepsilon_{gf}^{e} = \Delta\varepsilon_{gv} + \frac{\Delta p_{gf}}{K_m} - \Delta\varepsilon_{gs} \tag{16}$$

where ε_{gv} is the coal bulk strain.

As discussed above, $\Delta\varepsilon_{gf}^{int}$ results from the matrix non-uniform deformation. Due to the shortcomings of the conventional dual porosity/permeability approach, the matrix can only be regarded to be in an equilibrium state and will deform uniformly (Abbasi et al. 2019). The matrix strain ($\Delta\varepsilon_{gm}$) calculated from the deformation equation Eq. 7 only refers to the results when matrix is in uniform states. In this paper, we use the product of the non-equilibrium coefficient, obtained from the embedded local system, and the matrix strain under a uniform state (namely, $\gamma\Delta\varepsilon_{gm}$) to characterize the matrix strain under a non-uniform state. Meanwhile, we assume that the differential swelling volume between the matrix uniform and non-uniform deformation would fully contribute to changes in the fracture volume, that is, the mechanical matrix-fracture interaction. Therefore, according to the volumetric relation between matrix and fractures, namely $V_{gf}/V_{gm} = \varphi_{gf_0}/(1-\varphi_{gf_0})$ (Qu et al. 2014; Peng et al. 2014; Jiang et al. 2020), the following equation can be obtained:

$$\varphi_{gf_0}\Delta\varepsilon_{gf}^{int} = \left(1-\varphi_{gf_0}\right)\Delta\varepsilon_{gm} - \left(1-\varphi_{gf0}\right)\Delta\varepsilon_{gm}\gamma \tag{17}$$

where the first item on the right side of the equation refers to the matrix uniform swelling volume, while the second one refers to the matrix non-uniform swelling volume.

After rearrangement, the fracture strain induced by the matrix-fracture mechanical interaction can be expressed:

$$\Delta\varepsilon_{gf}^{int} = \frac{\left(1-\varphi_{gf_0}\right)(1-\gamma)\Delta\varepsilon_{gm}}{\varphi_{gf_0}} \tag{18}$$

In addition, the typical relationship between porosity and permeability is cubic law (Liu et al. 2011c). Therefore, coal permeability with the inclusion of the transient process in the matrix system can be expressed as:

$$\frac{k_{gf}}{k_{gf0}} = \left(1 + \frac{\alpha_f}{\varphi_{gf_0}}\left(\Delta\varepsilon_{gv} + \frac{\Delta p_{gf}}{K_m} - \Delta\varepsilon_{gs}\right) + \frac{\left(1-\varphi_{gf_0}\right)(1-\gamma)\Delta\varepsilon_{gm}}{\varphi_{gf_0}}\right)^3 \tag{19}$$

When the matrix deforms uniformly, that is, in the initial and ultimate equilibrium state, γ would be equal to unity, and the fracture strain induced by the mechanical interaction equals zero. Under this condition, Eq. 19 is the exact solution of conventional dual porosity/permeability models (Zhang et al. 2008; Liu et al. 2011a).

Different from the fracture system, in this study, the influence of the matrix non-uniform deformation on the matrix porosity is not considered. Therefore, the porosity of matrix is only defined as the function of the matrix effective strain.

$$\frac{\varphi_{gm}}{\varphi_{gm_0}} = 1 + \frac{a_m}{\varphi_{gm_0}}\Delta\varepsilon_{gm}^{e} \tag{20}$$

$$\Delta\varepsilon_{gm}^{e} = \Delta\varepsilon_{gm} + \frac{\Delta p_{gm}}{K_s} - \Delta\varepsilon_{gms} \tag{21}$$

According to the cubic law, the matrix permeability is:

$$\frac{k_{gm}}{k_{gm_0}} = \left(1 + \frac{\alpha_m}{\varphi_{gm_0}}\left(\Delta\varepsilon_{gm} + \frac{\Delta p_{gm}}{K_s} - \Delta\varepsilon_{gms}\right)\right)^3 \tag{22}$$

In the dual porosity/permeability approach, the rate of gas transfer between matrix and fractures is proportional to the pressure difference between two systems and can be described as the traditional mass exchange equation, as given by (Warren 1963; Ranjbar 2011).

$$q_{gt} = \frac{k_{gm}\rho}{\mu}\sigma\left(p_{gf} - p_{gm}\right) \tag{23}$$

where σ is called the matrix-fracture transfer shape factor and is related to matrix size, with dimension of L^{-2}.

Substituting Eqs. 11–23 into Eq. 10, the governing equations for gas flow in matrix and fractures can be described as

$$\left(\varphi_{gf}+\frac{p_b\rho_c V_L p_L}{(p_{gf}+p_L)^2}+\frac{a_f p_{gf}}{K_m}-\frac{a_f p_{gf}\varepsilon_L p_L}{(p_{gf}+p_L)^2}\right)\frac{\partial p_{gf}}{\partial t_g}+\nabla\left(-\frac{k_{gf}}{\mu}p_{gf}\nabla p_{gf}\right)=-a_f p_{gf}\frac{\partial\varepsilon_{gv}}{\partial t}-\frac{k_{gm}p_b}{\mu}\sigma(p_{gf}-p_{gm}) \tag{24}$$

$$\left(\varphi_{gm}+\frac{p_b\rho_c V_L p_L}{(p_{gm}+p_L)^2}+\frac{a_m p_{gm}}{K_s}-\frac{a_m p_{gm}\varepsilon_L p_L}{(p_{gm}+p_L)^2}\right)\frac{\partial p_{gm}}{\partial t_g}+\nabla\left(-\frac{k_{gm}}{\mu}p_{gm}\nabla p_{gm}\right)=-a_m p_{gm}\frac{\partial\varepsilon_{gm}}{\partial t}+\frac{k_{gm}p_b}{\mu}\sigma(p_{gf}-p_{gm}) \tag{25}$$

3.3 Cross-couplings

Through the above equations, the response of coal is controlled by fully coupled physical fields, consisting of the coal deformation, gas flow in matrix, gas flow in fractures and the pressure distribution within the matrix block. The first three belong to the global system, and the last to the local system. These fields are connected through a set of cross-coupling relations, as shown in Fig. 4. The detailed interactions are summarized as follows:

(a) The interaction between the coal deformation and gas flow in fractures refers to two terms: one is $\alpha_f p_{gf,i}$ and $K\varepsilon_{gfs,i}$, which means the coal deformation caused by changes in the effective stress on fractures and sorption-induced swelling of fractures. The other is the variation in fracture permeability induced by the coal deformation.

(b) The interaction between the coal deformation and gas flow in matrix refers to two terms: one is $\alpha_m p_{gm,i}$ and $K\varepsilon_{gms,i}$, which means the coal deformation caused by changes in the effective stress on matrix and sorption-induced swelling of matrix. The other is the variation in matrix permeability induced by the coal deformation.

(c) The interaction between gas flow in matrix and gas flow in fractures is defined term as two terms: $\frac{k_{gm}p_b}{\mu}\sigma(p_f-\overline{p_m})$ and $-\frac{k_m p_b}{\mu}\sigma(p_f-\overline{p_m})$, namely the mass transfer between two systems.

(d) The interactions among gas flow in matrix, gas flow in fractures, and the pressure distribution within the matrix block are defined as two terms: one is that pressure in matrix and fractures would influence the pressure distribution within the matrix block. The other is that the matrix non-uniform deformation induced by the pressure distribution would lead to the matrix-fracture interaction, affecting gas flow in fractures.

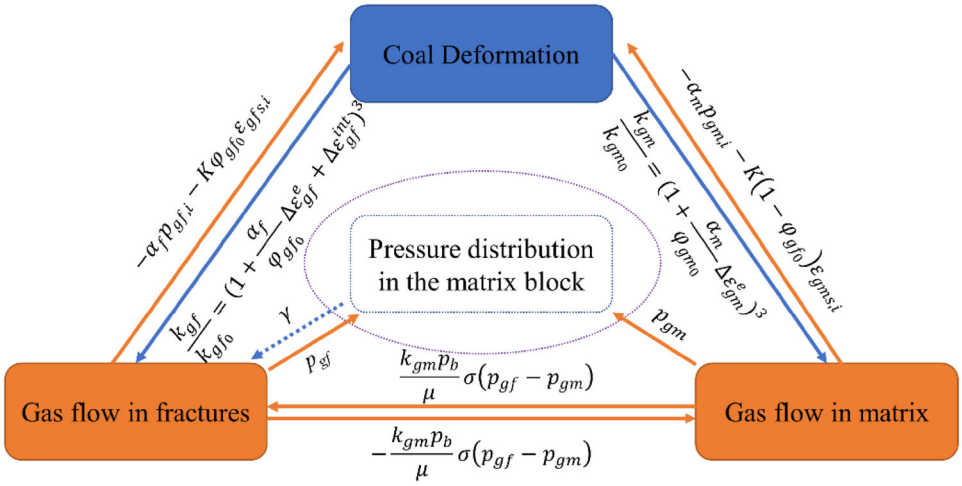

Fig. 4 Schematic defining cross-couplings among four physical fields: coal deformation, gas flow in matrix, gas flow in fractures and the pressure distribution within the matrix block

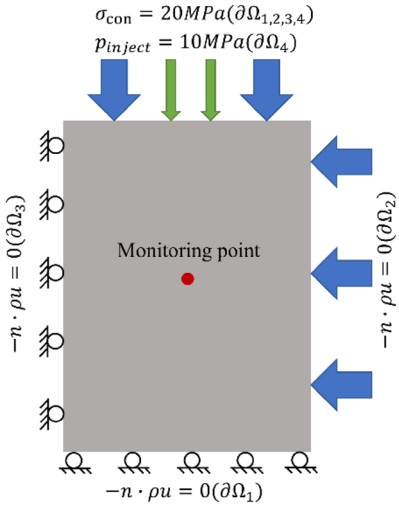

Fig. 5 Simulation model

4 Model verification

In this section, the proposed permeability model is verified through comparing the modelling results with the experimental ones (Siriwardane et al. 2009). In this experiment, a set of coal samples with artificial longitudinal fractures were used to investigate the influence of adsorbing gas exposure time on coal permeability. We collect experimental information from the original publication, and a case of the physical model is established according to the experimental condition, as shown in Fig. 5. The model size is 37.7 × 51.1 mm^2, where constant confining pressure is applied on the top and right boundaries while other boundaries are controlled by the roller constraint. Gas is injected from the top boundary while no flow is applied on remaining boundaries. The parameters used in the simulation come from this experiment and related studies (Zhang et al. 2008; Wu et al. 2010), which are listed in Table 1.

Table 1 Parameters of the simulation model

Parameter	Value
Initial matrix porosity	0.02
Initial fracture porosity	0.008
Young's modulus of matrix	8 [GPa]
Young's modulus of coal	4 [GPa]
Young's modulus of grains	10[GPa]
Possion's ratio	0.1
Dynamic viscosity	1.89×10^{-5} [Pa*s]
Biot coefficient of matrix	0.2
Biot coefficient of fracture	0.5
Initial matrix permeability	1.7×10^{-21} [m^2]
Initial fracture permeability	8×10^{-16} [m^2]
Coal density	1200 [kg/m^3]
Langmuir strain constant	0.04
Langmuir sorption capacity	0.0001 [m^3/kg]
Langmuir pressure constant	6.109 [MPa]
Shape factor	400 [m^{-2}]
Gas density	0.717 [kg/m^3]
Initial pressure	0.1 [MPa]
Gas compressibility	3.42^{-8}[Pa^{-1}]

The comparison between simulation results at the monitoring point and experimental ones is plotted in Fig. 6. The first data in the experiment was collected at 10 h and last one was collected at 220 h. The results show that permeability of the coal sample drops with the increase of exposure time within 80 h, and afterward it rebounds slowly until the end of the test. It is concluded that our new model captures the permeability evolution reasonably well. However, the evolution of the experimental permeability is only a small portion of the complete evolution process from initial to ultimate equilibrium.

In our model, coal consists of the matrix and fracture system. We define the equilibrium state for the fracture system as the global equilibrium, while that for the matrix system is the local equilibrium. The time to reach equilibrium states for two systems is defined as the global and local equilibrium time, respectively. Before the global equilibrium time is reached, the permeability evolution is controlled by the behavior of the fracture system. As the effective stress decreases, the fracture aperture becomes larger, and permeability rises. However, in the stage between the global and local equilibrium time, the matrix system plays a dominating role. During this period, initially, due to gas diffusion into matrix, matrix deforms non-uniformly, and the resulting matrix-fracture mechanical interaction compresses the fracture volume, resulting in a decrease in permeability. As gas further diffuses into matrix, the matrix deformation gradually transforms from non-uniform to uniform. The effect of the matrix system gradually weakens, and consequently permeability rebounds. Once the local equilibrium time is reached, the matrix

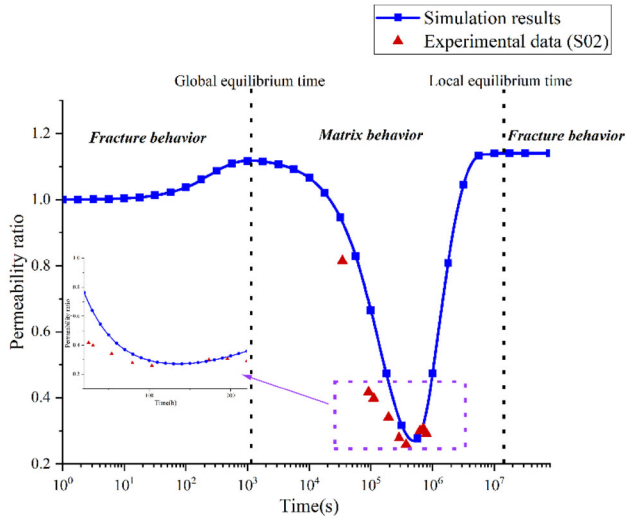

Fig. 6 Comparison between modelling results and experimental data

deformation is completely uniform, and the influence of the matrix system vanishes. Under this condition, permeability is controlled by the behavior of the fracture system again. And because of a reduction in the effective stress, coal permeability eventually is larger than initial value. As a tool of knowledge extension, our model restores a whole process of the coal permeability evolution based on the experimental data.

In equilibrium models, two equilibrium times are assumed to be the same and coal permeability is totally controlled by the fracture system. They underestimate the role of the matrix system. These models may be able to match experimental observations for conventional reservoirs since the difference between two equilibrium times is negligible. Due to the significant contrast between two equilibrium times for coal, the time-dependency of permeability under the influence of the transient process in matrix must be considered. Therefore, the coal permeability evolution is a phenomenon involving multi-spatial scales (matrix and fractures), multi-temporal scales (global and local equilibrium time), and multi-physics (gas flow and coal deformation).

5 Model applications

As discussed above, permeability evolutions for the experimental observations represent a small portion of the whole process. The majority of current laboratory measurements have been completed under the stress-controlled boundary conditions, which are divided into CES and CCP (Liu et al. 2011b; Wei et al. 2019a, b; Anggara 2016; Siriwardane 2009; Chen et al. 2011; Li et al. 2013; Wang et al. 2016; Feng et al. 2017). However, previous equilibrium models cannot

Table 2 Parameters used in the case of CES

Parameter	Value
Initial matrix porosity	0.02
Initial fracture porosity	0.018
Young's modulus of matrix	8 [GPa]
Young's modulus of coal	5 [GPa]
Young's modulus of grains	10[GPa]
Possion's ratio	0.1
Dynamic viscosity	1.89×10^{-5} [Pa*s]
Biot coefficient of matrix	0.2
Biot coefficient of fracture	0.375
Initial matrix permeability	1.25×10^{-21} [m^2]
Initial fracture permeability	0.9694×10^{-16} [m^2]
Coal density	1200 [kg/m^3]
Langmuir strain constant	0.0173
Langmuir sorption capacity	0.0001 [m^3/kg]
Langmuir pressure constant	2 [MPa]
Shape factor	800 [m^{-2}]
Gas density	0.717 [kg/m^3]
Initial pressure	0.5 [MPa]
Gas compressibility	3.42^{-8}[Pa^{-1}]

represent the whole evolution process under these conditions. In this section, we extend the concept of the permeability map proposed in the previous work (Zhang et al. 2018; Zeng et al. 2020). The proposed non-equilibrium model is applied to generate a set of coal permeability profiles to extend experimental data to the complete evolution process under CES and CCP conditions.

For CES cases, the experiment selected for analysis was conducted under a fixed effective stress of 2 MPa and gas injection pressure of 1 to 2.5 MPa (Anggara 2016). After continuously injecting gas into samples for at least 48 h, permeability data was collected. The parameter used in the simulation is listed in Table 2.

Based on simulation results, a 3D permeability map under CES conditions is generated, in which, X-axis refers to injection pressure, Y-axis refers to time, and Z-axis refers to the coal permeability ratio, as plotted in Fig. 7. Each slice parallel to the YZ-plane represents the permeability evolution over time under specific injection pressure. Once the permeability evolution on the YZ-plane is projected onto the XZ-plane, different permeability curves become vertical bars. After connecting the highest and lowest value of each vertical bar, two boundaries are obtained. The upper boundary is controlled by the behavior of the fracture system, and its value is equal to unity as the effective stress on fractures is constant. The lower boundary is dominated by the behavior of the matrix system, and its value drops with an increase in injection pressure. This is because the higher injection pressure is, the greater the degree of the matrix non-uniform deformation is, and the more obvious the resulting matrix-fracture interaction is.

The simulation results at 48 h under different gas injection pressure are also projected onto the XZ-plane and connected, as shown by the red long and short dash in Fig. 7. Obviously, the simulation results are in good agreement with the experimental ones. According to the prediction of the proposed model, the local equilibrium state is only reached after 1700 h. This indicates that the experiment tests were carried out at non-equilibrium states, instead of equilibrium states. In non-equilibrium states, due to the matrix-fracture

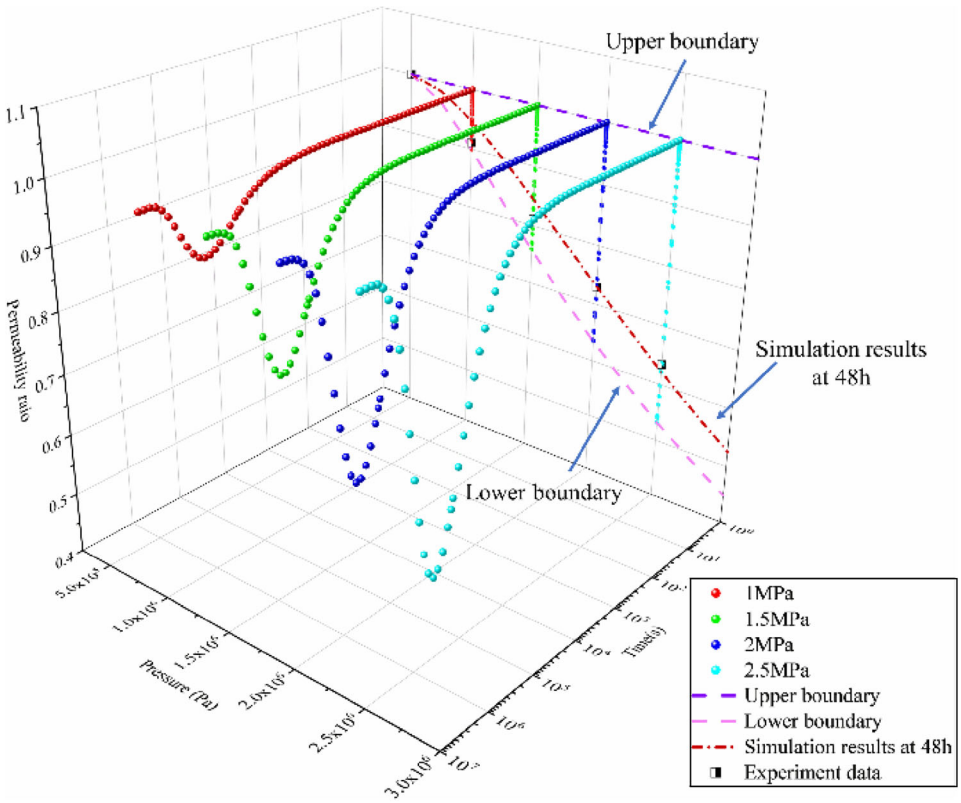

Fig. 7 3D permeability map under CES conditions

mechanical interaction, permeability is time-dependent and changes in a wide range. In other words, experimental data could appear anywhere between the two boundaries, depending on when the measurement is taken, and only constitutes a small portion of the whole evolution process. Through the proposed non-equilibrium model, the experimental data is extended to the whole evolution process under CES conditions, where permeability ratios change within two envelopes.

For CCP cases, we analyze data from the experiment conducted by Li in 2013, where confining pressure was set to remain unchanged (4.3 MPa) and gas injection pressure was set from 0.5 to 4.1 MPa (Li et al. 2013). The input parameters for simulation are collected from the original literature (listed in Table 3). A 3D permeability map under CCP conditions is plotted in Fig. 8. Like CES cases, under CCP conditions, permeability ratios are also bounded within two envelopes. The upper and lower boundary are determined by the behavior of the fracture system and the matrix system, respectively. In this experiment, the measured time is not given. It is impossible to directly know whether the experimental observations were conducted in equilibrium states. However, if the measurements were conducted after the local equilibrium time, the matrix system would play a trivial role. The permeability evolution should be only controlled by the fracture system and be coincided with the upper boundary. Nevertheless, the experimental observations are located between two boundaries and drop with an increase in gas injection pressure. Therefore, the experiment in the literature was also conducted in non-equilibrium states, and due to the influence of the transient process in matrix, permeability changes dramatically. In this case, it is difficult to predict or explain experimental observations by a single line, while a permeability map with two bounds can include all possibilities about experimental data under CCP conditions.

Table 3 Parameters used in the case of CCP

Parameter	Value
Initial matrix porosity	0.02
Initial fracture porosity	0.0045
Young's modulus of matrix	8 [GPa]
Young's modulus of coal	6 [GPa]
Young's modulus of grains	10[GPa]
Possion's ratio	0.1
Dynamic viscosity	$1.89*10^{-5}$ [Pa*s]
Biot coefficient of matrix	0.2
Biot coefficient of fracture	0.25
Initial matrix permeability	1.7×10^{-21} [m^2]
Initial fracture permeability	0.48×10^{-18} [m^2]
Coal density	1200 [kg/m^3]
Langmuir strain constant	0.04
Langmuir sorption capacity	0.0001 [m^3/kg]
Langmuir pressure constant	1.1 [MPa]
Shape factor	800 [m^{-2}]
Gas density	0.717 [kg/m^3]
Initial pressure	0.5 [MPa]
Gas compressibility	3.42^{-8}[Pa^{-1}]

6 Conclusions

Conventional dual porosity/permeability models do not consider the transient nature of an individual process such as diffusion within an REV (representative elementary volume). The REV is treated as a mathematical construct rather than a physical entity. For low permeability coal, this may result in significant inconsistencies between conventional theory and lab & field observations as reported widely in the current literature. In this study, the theoretical deficiency has been addressed through the embedment of a local REV structure into the overall multiphysics formulation. This inclusion has transformed conventional dual porosity/permeability equilibrium models into non-equilibrium ones. Consequently, coal permeability evolves also from an initial to a final equilibrium. Equilibrium models represent two end points (initial and final equilibrium) while our new model represents the evolution of coal permeability between these two end points. Specific conclusions are summarized in the following:

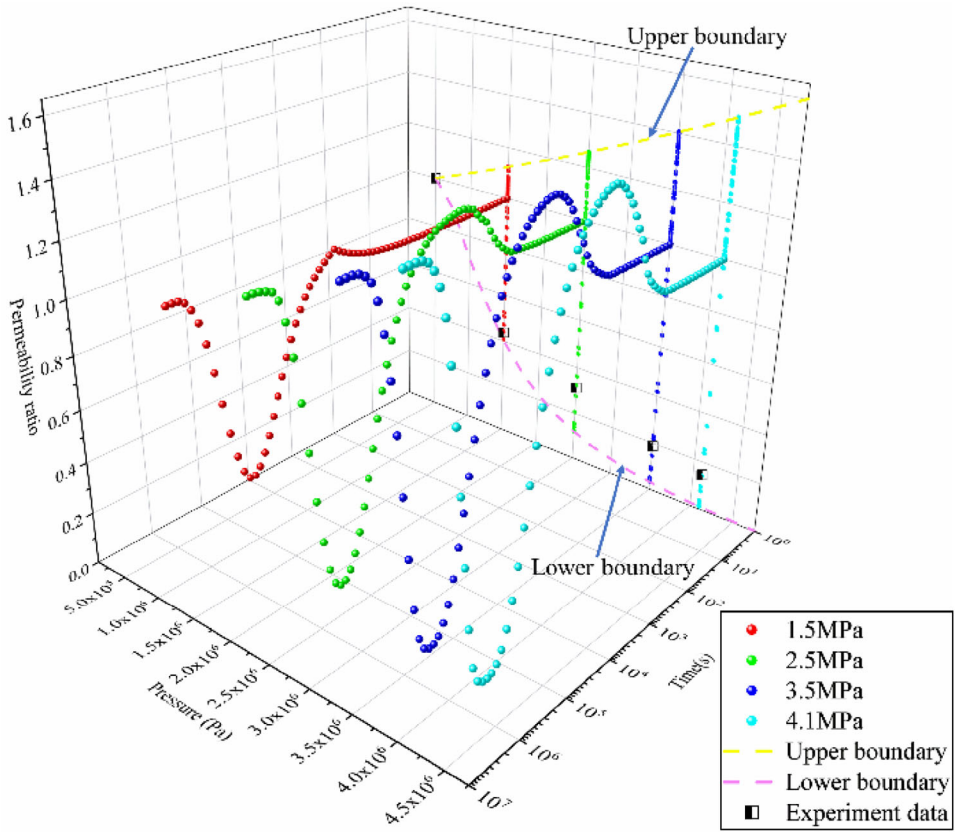

Fig. 8 3D permeability map under CCP conditions

For a typical dual porosity/permeability coal, the transient nature of an individual process, such as diffusion within the matrix in an REV, must be considered. Neglecting this mechanism in conventional models is a primary reason for the discrepancy between theoretical predictions and lab or field observations.

The inclusion of transient processes in the matrix system into an overall multiphysics framework has transformed conventional dual porosity/permeability models from equilibrium to non-equilibrium models. This transformation is important particularly for low permeable rocks such as coal and shale because of the huge contrast between fracture and matrix properties.

Acknowledgements This work is supported by the Australian Research Council under Grant DP200101293. The first author is supported by the UWA-China Joint Scholarships. These supports are gratefully acknowledged.

References

Abbasi M, Kazemi A, Sharifi M (2019) Modeling of transient shape factor in fractured reservoirs considering the effect of heterogeneity, pressure-dependent properties and quadratic pressure gradient. Oil Gas Sci Technol–Rev d'IFP Energ Nouv 74(5):89

Anggara F, Sasaki K, Sugai Y (2016) The correlation between coal swelling and permeability during CO2 sequestration: a case study using Kushiro low rank coals. Int J Coal Geol 166:62–70

Barenblatt GI (1960) Basic concepts in the theory of seepage of homogeneous liquids in fissured rocks. Prikl Mat Mekh 24(5):852–864

Bear, J., 2013. Dynamics of fluids in porous media. Courier Corporation.

Berre I, Doster F, Keilegavlen E (2019) Flow in fractured porous media: a review of conceptual models and discretization approaches. Transp Porous Media 130(1):215–236

Cao P, Liu J, Leong YK (2016) General gas permeability model for porous media: bridging the gaps between conventional and unconventional natural gas reservoirs. Energy Fuels 30(7):5492–5505

Chen Z, Liu J, Elsworth D, Connell L, and Pan Z, 2009 Investigation of CO2 injection induced coal-gas interactions. In:

43rd US Rock Mechanics Symposium & 4th US-Canada Rock Mechanics Symposium. American Rock Mechanics Association.

Chen Z, Pan Z, Liu J, Connell LD, Elsworth D (2011) Effect of the effective stress coefficient and sorption-induced strain on the evolution of coal permeability: experimental observations. Int J Greenhouse Gas Control 5(5):1284–1293

Cheng AHD (2016) Poroelasticity, vol 27. Springer International Publishing, Switzerland

Cui X, Bustin RM (2005) Volumetric strain associated with methane desorption and its impact on coalbed gas production from deep coal seams. AAPG Bull 89(9):1181–1202

Farah N, Delorme M, Ding DY, Wu YS, Codreanu DB (2019) Flow modelling of unconventional shale reservoirs using a DFM-MINC proximity function. J Petrol Sci Eng 173:222–236

Feng R, Harpalani S, Pandey R (2017) Evaluation of various pulse-decay laboratory permeability measurement techniques for highly stressed coals. Rock Mech Rock Eng 50(2):297–308

Gray I (1987) Reservoir engineering in coal seams: Part 1-The physical process of gas storage and movement in coal seams. SPE Reserv Eng 2(01):28–34

Jiang C, Zhao Z, Zhang X, Liu J, Elsworth D, Cui G (2020) Controlling effects of differential swelling index on evolution of coal permeability. J Rock Mech Geotech Eng 12(3):461–472

Li J, Liu D, Yao Y, Cai Y, Chen Y (2013) Evaluation and modeling of gas permeability changes in anthracite coals. Fuel 111:606–612

Lim KT, Aziz K (1995) Matrix-fracture transfer shape factors for dual-porosity simulators. J Petrol Sci Eng 13(3–4):169–178

Liu HH, Rutqvist J (2010) A new coal-permeability model: internal swelling stress and fracture–matrix interaction. Transp Porous Media 82(1):157–171

Liu J, Chen Z, Elsworth D, Miao X, Mao X (2011a) Evolution of coal permeability from stress-controlled to displacement-controlled swelling conditions. Fuel 90(10):2987–2997

Liu J, Chen Z, Elsworth D, Qu H, Chen D (2011b) Interactions of multiple processes during CBM extraction: a critical review. Int J Coal Geol 87(3–4):175–189

Liu J, Wang J, Chen Z, Wang S, Elsworth D, Jiang Y (2011c) Impact of transition from local swelling to macro swelling on the evolution of coal permeability. Int J Coal Geol 88(1):31–40

Moore TA (2012) Coalbed methane: a review. Int J Coal Geol 101:36–81

Palmer, I and Mansoori J, 1996. How permeability depends on stress and pore pressure in coalbeds: a new model. In: SPE annual technical conference and exhibition. Society of Petroleum Engineers.

Pan Z, Connell LD (2012) Modelling permeability for coal reservoirs: a review of analytical models and testing data. Int J Coal Geol 92:1–44

Patzek TW, Male F, Marder M (2013) Gas production in the Barnett Shale obeys a simple scaling theory. Proc Natl Acad Sci 110(49):19731–19736

Patzek T, Male F, Marder M (2014) A simple model of gas production from hydrofractured horizontal wells in shales. AAPG Bull 98(12):2507–2529

Peng Y, Liu J, Pan Z, Connell LD, Chen Z, Qu H (2017) Impact of coal matrix strains on the evolution of permeability. Fuel 189:270–283

Peng Y, Liu J, Wei M, Pan Z, Connell LD (2014) Why coal permeability changes under free swellings: new insights. Int J Coal Geol 133:35–46

Qu H, Liu J, Pan Z, Connell L (2014) Impact of matrix swelling area propagation on the evolution of coal permeability under coupled multiple processes. J Natural Gas Sci Eng 18:451–466

Ranjbar E, Hassanzadeh H (2011) Matrix–fracture transfer shape factor for modeling flow of a compressible fluid in dual-porosity media. Adv Water Resour 34(5):627–639

Shi R, Liu J, Wang X, Elsworth D, Liu Z, Wei M, Liu X, Wang Z (2020) Experimental observations of heterogeneous strains inside a dual porosity sample under the influence of gas-sorption: a case study of fractured coal. Int J Coal Geol 223:103450

Shi JQ, Durucan S (2014) Modelling laboratory horizontal stress and coal permeability data using S&D permeability model. Int J Coal Geol 131:172–176

Shi JQ, Durucan S (2005) A model for changes in coalbed permeability during primary and enhanced methane recovery. SPE Reservoir Eval Eng 8(04):291–299

Shi R, Liu J, Wei M, Elsworth D, Wang X (2018) Mechanistic analysis of coal permeability evolution data under stress-controlled conditions. Int J Rock Mech Min Sci 110:36–47

Siriwardane H, Haljasmaa I, McLendon R, Irdi G, Soong Y, Bromhal G (2009) Influence of carbon dioxide on coal permeability determined by pressure transient methods. Int J Coal Geol 77(1–2):109–118

Tan Z, Wang S, Ma L (2011) Current status and prospect of development and utilization of coal mine methane in China. Energy Procedia 5:1874–1877

Wang C, Liu J, Feng J, Wei M, Wang C, Jiang Y (2016) Effects of gas diffusion from fractures to coal matrix on the evolution of coal strains: Experimental observations. Int J Coal Geol 162:74–84

Warren JE, Root PJ (1963) The behavior of naturally fractured reservoirs. Soc Petrol Eng J 3(03):245–255

Wei M, Liu J, Elsworth D, Li S, Zhou F (2019a) Influence of gas adsorption induced non-uniform deformation on the evolution of coal permeability. Int J Rock Mech Min Sci 114:71–78

Wei M, Liu J, Feng X, Wang C, Zhou F (2016) Evolution of shale apparent permeability from stress-controlled to displacement-controlled conditions. J Natural Gas Sci Eng 34:1453–1460

Wei M, Liu J, Shi R, Elsworth D, Liu Z (2019b) Long-term evolution of coal permeability under effective stresses gap between matrix and fracture during CO 2 injection. Transp Porous Media 130(3):969–983

Wu YS, Pruess K (1988) A multiple-porosity method for simulation of naturally fractured petroleum reservoirs. SPE Reserv Eng 3(01):327–336

Wu Y, Liu J, Elsworth D, Chen Z, Connell L, Pan Z (2010) Dual poroelastic response of a coal seam to CO2 injection. Int J Greenhouse Gas Control 4(4):668–678

Zeng J, Liu J, Li W, Leong YK, Elsworth D, Guo J (2020) Evolution of shale permeability under the influence of gas diffusion from the fracture wall into the matrix. Energy Fuels 34(4):4393–4406

Zhang H, Liu J, Elsworth D (2008) How sorption-induced matrix deformation affects gas flow in coal seams: a new FE model. Int J Rock Mech Min Sci 45(8):1226–1236

Zhang S, Liu J, Wei M, Elsworth D (2018) Coal permeability maps under the influence of multiple coupled processes. Int J Coal Geol 187:71–82

Zhao Y, Hu Y, Zhao B, Yang D (2004) Nonlinear coupled mathematical model for solid deformation and gas seepage in fractured media. Transp Porous Media 55(2):119–136